Soft Matter

PAPER

View Article Online
View Journal

Cite this: DOI: 10.1039/c7sm00978j

Propagation of a thermo-mechanical perturbation on a lipid membrane

M. I. Pérez-Camacho and J. C. Ruiz-Suárez *

Received 17th May 2017,
Accepted 31st August 2017

DOI: 10.1039/c7sm00978j

rsc.li/soft-matter-journal

The propagation of sound waves on lipid monolayers supported on water has been previously studied during the melting transition. Since changes in volume, area, and compressibility in lipid membranes have biological relevance, the observed sound propagation is of paramount importance. However, it is unknown what would occur on a lipid bilayer, which is a more approximate model of a cell membrane. With the aim to answer this relevant question, we built an experimental setup to assemble long artificial lipid membranes. We found that if these membranes are heated in order to force local melting, a thermo-mechanical perturbation propagates a long distance. Our findings may support the existence of solitary waves, postulated to explain the propagation of isentropic signals together with the action potential in neurons.

1 Introduction

Cells are enclosed by lipid membranes, complex structures responsible for providing integrity and controlling the flux of substances through them. In addition, membranes are also a vehicle for the propagation of information, for example in specialized cells called neurons. Many reports have proposed different models of cell membranes to explain how the propagation of information, materialized in a signal called action potential, takes place and the function that its components have in the process. This is essential in the Hodgkin–Huxley model (H–H),[1] which considers the action potential as an electrical phenomenon induced by the flow of ions through protein channels, where the lipid membrane acts as a capacitor. Although the H–H model is the benchmark in neuroscience, there are some non-electrical events that cannot be explained in terms of ions flows. In nerves, the action potential is accompanied by mechanical displacements[2–4] as well as adiabatic changes in temperature.[4–8] This, of course, is at odds with the fact the action potential is a dissipative process produced by the diffusion of ions through protein channels.

Moreover, it is well known that electrical, mechanical and thermodynamic properties occur in lipid membranes[9,10] and a wide variety of biological systems exhibit spontaneous mechanical perturbations associated with electrical events[4] and melting transitions below body temperature.[11–13] The volume and area changes in lipid membranes have a close relationship with pressure and temperature:[14–17] in a 1,2-dipalmitoyl-*sn-glycero*-3-phosphocholine (DPPC) lipid membrane, the volume change from the gel to liquid phase is nearly 4%,[12,18,19] while the lipid area varies by 25%[20] and the thickness decreases by about 16%.[12] During the phase transition it is known that the heat capacity, c_P, the permeability of the membrane, and the relaxation times display maximum values. Besides, the membrane becomes softer when it is compressed, and the volume k^V and area k^A compressibilities reach a maximum.[21–23] During the phase transition, the speed of sound, $c = 1/\sqrt{k_s^V \rho^A}$, is a function of adiabatic compressibility and is also frequency dependent.[12,23] In the low frequency regime, the adiabatic compressibility approaches the isothermal compressibility $k_s \approx k_T$, and the speed of a mechanical wave travelling along a membrane is $c = 1/\sqrt{k_T^A \rho^A}$. Both the dependence of c on frequency and the increase of compressibility in the lipid melting transition are necessary conditions for the propagation of solitary pulses. With regard to this idea, Heimburg and Jackson, based on previous works, proposed a model where the propagation of a solitary wave can be achieved by bringing a tiny section of the fluid membrane into the gel phase.[12] Indeed, near the phase transition a local change in temperature,[24] a sudden change in pH,[25] a local increase in calcium concentration[26] or an electrostatic potential,[13,27] could trigger this pulse.

The first study carried out to show the possibility of this phenomenon was performed on a lipid monolayer,[28] where the thermodynamic state is easily modified by lateral pressure on a Langmuir balance.[29] It has been shown that in this system, the propagation of acoustic pulses can be triggered by small amounts of solvents released onto the monolayer surface.[28] Also, the first evidence of solitary pulses on a lipid Langmuir monolayer and their dependence on the thermodynamic parameters were recently shown near the phase transition.[30,31] These works demonstrate the relationship between such pulses

CINVESTAV-Monterrey, Autopista Nueva al Aeropuerto Km. 9.5, Apodaca, Nuevo León 66600, Mexico. E-mail: jcrs.mty@gmail.com

and the state of the lipid interface, agreeing with the soliton model originally proposed by Heimburg and Jackson.

Nevertheless, from a biological perspective, a system that better resembles a real membrane is a lipid bilayer supported by a hydrophobic surface under water. The technique used to assemble such bilayers is called a black lipid membrane (BLM). In the BLM, the diameter of the orifice where the bilayer is normally supported does not surpass 250 μm.[32] Although large enough to study many electrical and elastic properties, such a short bilayer is inadequate to test the possible existence of a solitary wave. To circumvent this restriction, we designed an experimental setup to assemble lipid membranes comparable in length to a large real neuron (0.1 m). Then, we carry out experiments where the membranes are locally heated within a tiny region. Far away from such a region, we optically measured the arrival of a mechanical perturbation, presumably triggered by the thermal input. This observation provides further support to the idea that solitons do exist in real neurons.

2 Materials and methods

n-Decane, chloroform, methanol, *n*-hexadecane and *n*-pentane were obtained from Sigma Aldrich. 1,2-Dimyristoyl-*sn-glycero*-3-phosphocholine (DMPC) and 1,2-dipalmitoyl-*sn-glycero*-3-phosphocholine (DPPC) were purchased from Avanti Polar Lipids (Birmingham, AL) and used without further purification. Lipid solutions (20 mg ml^{-1}) in 7 : 2 : 1 *n*-decane/chloroform/methanol were prepared and agitated for 20 minutes in order to achieve a homogeneous mixture. For all experiments, purified water was used.

Fig. 1 depicts the lipid membrane system built to perform the experiments. It consists of an anodized aluminium block that is heated by circulating water (6). A system of parallel acrylic plates (1,3) is embedded in the block and it divides this block into two chambers. Each one has a water valve and an electrode connection (4,5). The linear lipid membrane is painted on a slit made on an acetate sheet (2). The slit is 10.0 cm in length and 200 μm in width and is held in the middle by the acrylic plates. In each experiment, the acetate sheet was cleaned and then pre-painted with 5% *n*-hexadecane in *n*-pentane in order to reduce the mechanical tension at the edges of the aperture. The sandwich (acrylic plates and acetate sheet) was carefully lowered inside the block. The chambers were filled with purified water. After the chosen temperature is reached and the system is in equilibrium, 20 mg ml^{-1} lipid solution in 7 : 2 : 1 *n*-decane/chloroform/methanol is deposited along the slit employing a micropipette. Ag/AgCl electrodes were placed previously in each compartment and then connected to an electrometer (6517b, Keithley Instruments, Inc). The formation of membranes was controlled visually and by electrical measurements with a triangular 100 mV voltage input pulse in order to verify the correct sealing of the membranes and the moment of their rupture.

Since the aim of this work was to propagate a mechanical perturbation along lipid membranes due to a phase transition, we first need to know their melting temperatures (T_m). DPPC and DMPC have the following T_ms: 41 and 24 °C. However, the deposited mixtures contain solvents that do change these temperatures. In order to know their new values, we ought to perform a calorimetry analysis. Heat capacity profiles were recorded at a constant scan rate of 1 °C min^{-1} and constant pressure of 3 atm. The lipid concentration was also 20 mg ml^{-1} dissolved in 7 : 2 : 1 *n*-decane/chloroform/methanol. A calorimeter (Microcalorimeter, NanoDSC, TA Instrument) was interfaced to a PC, and data were analysed using the software provided with the instrument. Then, the solution was dissolved in water (to induce the formation of vesicles). The suspension was stirred at 500 rpm for 30 min above the T_m. Finally, the sample was centrifuged at 10 000 rpm (G-force of 10 621 × *g*) in an Eppendorf centrifuge 5804R, with a F-45-30-11 rotor for 10 min, and the supernatant was removed in order to eliminate the excess of solvent. For experiments without solvent, 3 mg ml^{-1} of lipid were hydrated

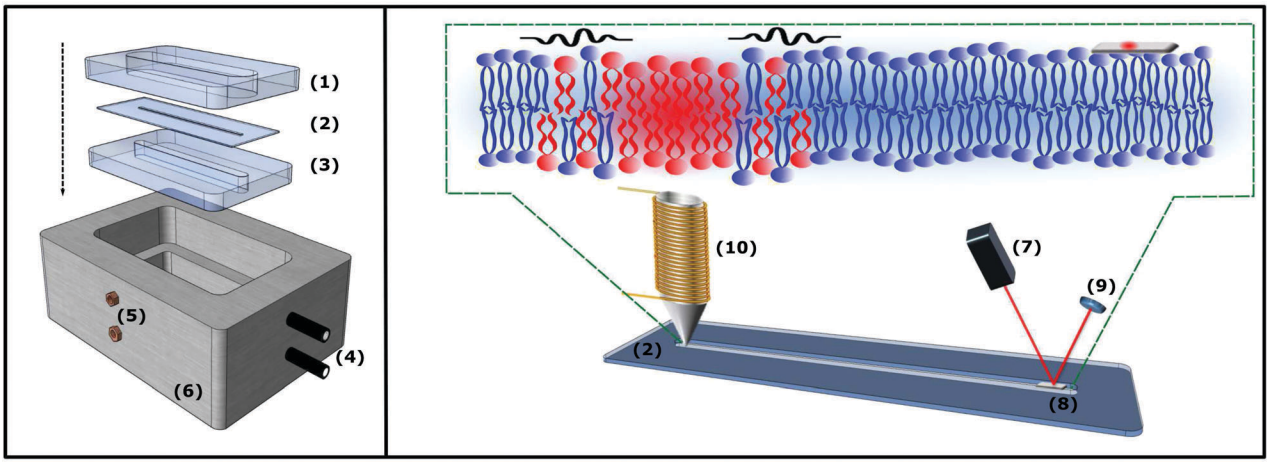

Fig. 1 Experimental setup. (left) A schematic drawing of the chamber: (1) acrylic top plate, (2) acetate film with the aperture, (3) acrylic bottom plate, (4) water inlet valves, (5) Ag/AgCl electrode connection, (6) solid aluminium chamber. (right) A schematic darwing of the lipid membrane, heating and optical detector: (7) light source, (8) Mylar target, (9) photodetector and (10) hot tip.

with Milli-Q-water and stirred for 30 min at 50 °C. In all samples, small unilamellar vesicles (SUVs) were subsequently obtained by extrusion through a polycarbonate filter of a pore size of 100 nm. Each experiment was equilibrated during 600 s at 2 °C. A heating scan from 2 to 50 °C was performed and was followed by a cooling scan. This cycle was repeated 3 times for each sample. Since all the previous scans do not show differences, only the third scan is presented.

The trigger/detection system consists of two parts separated by a distance of 10 cm, see Fig. 1: a heatable conical tip and an optical mirror where a laser beam is deflected. A hollow cone with a very sharp tip (diameter 100 microns) is machined at the end of an aluminium cylinder, which is coiled with a thin copper wire (10). The wire ends are connected to a voltage source. When the current flows, the wire heats and the tip of the cone is warmed up to a constant temperature measured by a thermocouple. The cylindrical cone is connected to a high precision micrometer in order for the tip to eventually touch the membrane with accuracy. In each experiment, the conical tip makes contact with the suspended membrane at one of its ends, see the right panel of Fig. 1. Next, in order to measure a possible change in the lipid bilayer thickness at the inspection point, far away from the hot tip, an optical detector is used. After the bilayer is formed on the slit, a very tiny polyethylene terephthalate target (reflective Mylar), weighing approximately 5 μg, is carefully placed onto the membrane (8). A laser beam (wavelength 632.8 nm) (7) is reflected on such mirror. A two-segment photodiode (9) senses the reflected beam, and this light signal produces a voltage, which is then amplified by a lock-in amplifier (HF2LI Lock-in Amplifier, Zurich Instruments AG) to improve the signal-to-noise ratio. Any perturbation of the membrane causes a change in the target position because the mirror can move freely. If the mechanical perturbation is large enough, it throws the Mylar away from its position, producing a signal voltage that cannot be recovered.

3 Results and discussion

Fig. 2 displays how the presence of solvents (in our case *n*-decane, chloroform, and methanol, necessary for providing stability in such large bilayers) induces shifts in the melting transition of membranes. Indeed, compared to the T_ms of SUVs of pure lipids, the shifts are very large. For DPPC, the solvent-free SUVs display a principal peak at 41 °C. The addition of the organic solvents during the process of preparation results in a rather small peak at a much lower temperature (30.7 °C). Analogously, for solvent-free DMPC vesicles the T_m is 24 °C and once the solvents are added the peak attenuates and displaces to the left (14.6 °C). Our results are in agreement with reports stating that the presence of short-chain alkanes in DPPC membranes decreases the melting temperature and broadens the transition.[33–37] During the experiment, it is not possible to determine with precision the melting temperature of the BLM. This is due in large to two aspects: first, the evaporation of solvent can promote a shift in the melting temperature and second, the curvature of the lipid

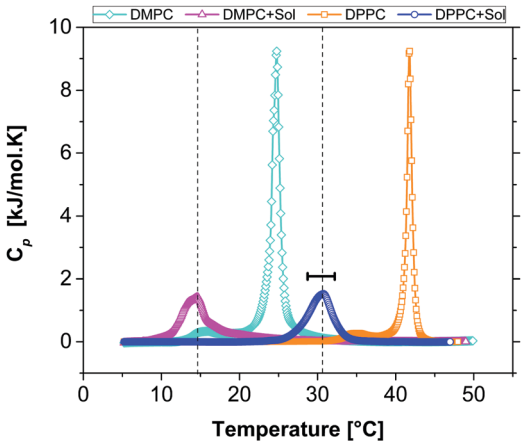

Fig. 2 Calorimetric study of DPPC and DMPC liposomes and the effect of solvents on the calorimetric profiles. Yellow squares correspond to control liposomes of DPPC at 3 mg ml^{-1}. Blue circles correspond to *n*-decane/chloroform/methanol in liposomes of DPPC. Cyan diamonds correspond to control liposomes of DMPC at 3 mg ml^{-1}. Magenta triangles show the effect of solvents on the temperature transition of liposomes of DMPC. The data correspond to the third scan in heating mode for each sample. Dashed lines mark the temperature transition shifts, which are approximately $|\Delta T_m|$ = 10 °C.

bilayer plays an important role in the phase transition behaviour.[38,39] In a BLM system, a narrower heat capacity profile and shifted tenths of a degree are expected in comparison to vesicles of the same lipids. However, we consider the melting temperature near to the one shown in DSC experiments. In Fig. 2, the dashed lines mark the transition temperatures of the membranes with solvents.

For reasons that we are going to clarify later, the temperature of the chamber is set at 25 °C (for DPPC) and 35 °C (for DMPC). Once the membranes are painted under water, the electrical capacitance and current display an important decrease. Fig. 3 shows the electrical measurements for 5 different bilayers during their formation process. The amount of solvent after painting produces differences in the width of the bilayer displayed as a standard deviation. The formation of lipid bilayers is a spontaneous and self-assembly process. It is very well known that the membrane formation is a self-sealing process because a hole in a bilayer is energetically unfavorable.[40]

The stability of the lipid bilayers is then analysed, finding that they can last without rupture for 40 minutes, long enough to prepare and carry out the experiments. The tiny piece of Mylar is gently deposited onto the membrane as observed in Fig. 1. Thereafter, the laser and detector are aligned, as assessed by the maximum voltage output V_0 given by the amplifier. Once the alignment is performed, the conical tip is lowered at the other end of the membrane until it makes contact with it. Fortunately for us, the bilayer withstands the weight and no rupture, as measured by the electrical current, is observed. The heater is turned on and the temperature of the metallic cone increases steadily, heating in turn the membrane just below the tip (as previously measured by a thermocouple), see the magenta line (squares) in Fig. 4(a). It is important to remark

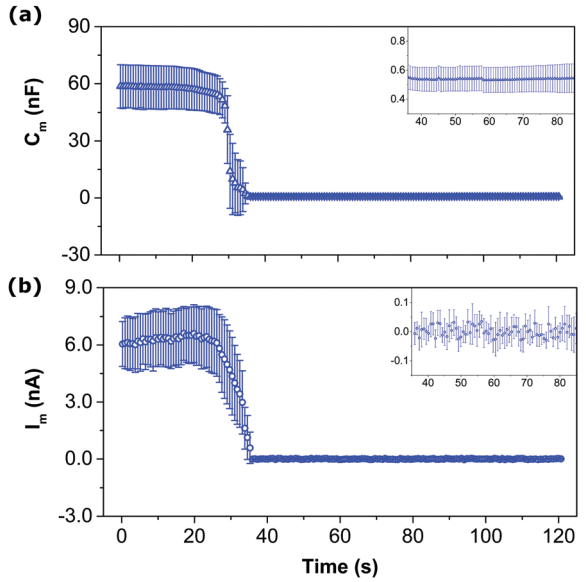

Fig. 3 Electrical response of the system during lipid membrane painting at T = 25 °C. (a) Blue triangles correspond to capacitance measurement in a DPPC lipid bilayer. (b) Blue circles show the effect of the DPPC lipid membrane on the current registered by the electrodes in the chamber. The insets show the capacitance and current values reached when the membrane is formed. Vertical lines mark the standard deviation for n = 5.

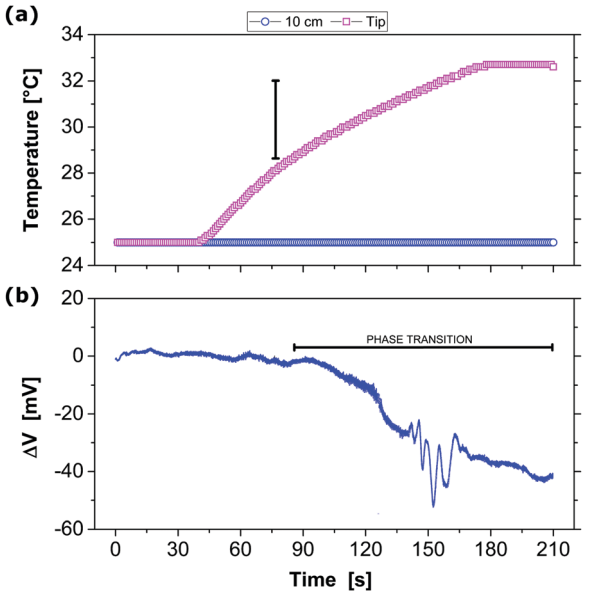

Fig. 4 Temperature and voltage measurements during the experiment. The black lines correspond to the range in which the phase transition of the vesicles in the calorimeter occurs (see Fig. 2). (a) The temperature on the tip (submerged in water), as a function of time, is given by the magenta curve (squares). We note that it takes a bit more than two minutes for the coil to increase the temperature from the bath temperature to 33 °C. The blue line (circles) corresponds to the temperature at which the Mylar target is positioned. (b) Representative voltage trace produced by the photodiode as a function of time for a DPPC bilayer. ΔV is the difference between the voltage output and its initial value V_0. The change in the voltage signal is produced during the phase transition.

that the temperature of the water around the piece of Mylar (10 cm away from the hot tip), never senses an augment of temperature, see blue line (circles) in Fig. 4(a).

As mentioned before, the temperature of the whole system (water and membrane) is 25 °C (for DPPC). When the local temperature of the membrane (below the tip) reaches 28.7 °C, two degrees below the transition temperature of DPPC/solvents depicted in Fig. 2 (30.7 °C), ΔV substantially descends as shown in Fig. 4(b) and 5. This means that the laser spot loses its alignment with the photodiode. Clearly, such misalignment must be caused by a change in the position of the supported Mylar. The fact that this response is associated with the phase transition (marked by black lines in Fig. 2, 4, and 5) hints towards the following episode: the membrane below the tip melts and the thickness and lateral density (ρ^A) decrease locally. Indeed, lipids below and around the tip increase the temperature near T_m. This transition propagates along the membrane reaching the position where the Mylar is located.

We now see the case of DMPC. According to Fig. 2, its gel–fluid transition occurs at 14.6 °C. Such a low temperature allows us to use it as a control experiment. To stay well above the transition, this time we increase the temperature of the bath up to 35 °C. Next, the membrane is locally heated with the conical tip from 35 to 42 °C. In the inset of Fig. 5, we show the results for three experiments. Note that ΔV is constant, meaning that the Mylar is never perturbed. In other words, since the membrane remained in the same fluid phase, no expansion is observed. From this control experiment, we also deduce that there is no significant change in the volume of water or metal expansion of the tip during heating that could affect the measurement.

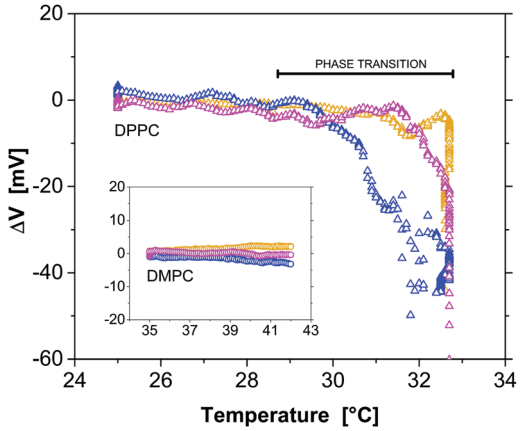

Fig. 5 Combining figures a and b in Fig. 4, we obtain the voltage as a function of temperature on the tip. Data for three experiments for DPPC are depicted. The black line corresponds to the phase transition observed in Fig. 2. Data for three experiments for DMPC are shown in the inset. See the explanation in the main text.

Theoretical considerations

Next, we would like to show that our results are in accordance with the soliton model proposed by Heimburg and Jackson.[12] This model is based on the wave equation for sound propagation in one dimension:

$$\frac{\partial}{\partial \tau^2}\Delta\rho^A = \frac{\partial}{\partial z}\left(c^2\frac{\partial}{\partial z}\Delta\rho^A\right) - h\frac{\partial^4}{\partial z^4}\Delta\rho^A, \quad (1)$$

with

$$c^2 = \frac{1}{\rho^A k_T^A} = c_0^2 + p\Delta\rho^A + q(\Delta\rho^A)^2, \quad (2)$$

where the lateral density is a function of the coordinate z and time τ.

The parameters p and q describe the non-linear elastic properties of the membrane and they are obtained by fitting experimental values. For a lipid membrane in the fluid phase, at a temperature above the melting transition, $\Delta\rho^A = \rho^A - \rho^A_{fluid} > 0$ and this requires that $p < 0$ and $q > 0$. The analytic solution of eqn (1), with $u = \frac{\Delta\rho^A}{\rho^A_{fluid}}$, was shown by Lautrup *et al.*[41] to be:

$$u(\xi) = \frac{2a_+a_-}{(a_+ + a_-) + (a_+ - a_-)\cosh\left(\xi\sqrt{1-\beta^2}\right)}, \quad (3)$$

with two real roots:

$$a\pm = -\frac{B_1}{B_2}\left(1 \pm \sqrt{\frac{\beta^2 - \beta_0^2}{1-\beta_0^2}}\right). \quad (4)$$

For $1 > |\beta| > \beta_0 = \sqrt{1 - \frac{B_1^2}{6B_2}}$, $B_1 = \frac{\rho^A_{fluid}}{c_0^2}p$, and $B_2 = \frac{{\rho^A_{fluid}}^2}{c_0^2}q$.

At minimum velocity β_0, the soliton has the maximum amplitude. For the unilamellar DPPC case at 45 °C, ρ^A_{fluid} = 4.035 × 10^{-3} g m^{-2}, c_0 = 176.6 m s^{-1},[12] B_1 = −16.6 and B_2 = 79.5.[12,41]

When the membrane is in the gel state, $\Delta\rho^A = \rho^A - \rho^A_{gel} < 0$, p and q must be >0. Considering that the lateral sound velocity c^2 has a minimum during the transition,[21,30] we can fit the new data in eqn (2) with the values reported at T = 45 °C[12] and obtain different parameters for the membrane below the melting temperature, see Fig. 6.

The new values for DPPC vesicles are ρ^A_{gel} = 4.877 × 10^{-3} g m^{-2}, c_0 = 177.2 m s^{-1}, $p = 20.01\frac{c_0^2}{\rho^A_{gel}}$ and $q = 115.4\frac{c_0^2}{{\rho^A_{gel}}^2}$, at a bulk temperature around 38 °C. Using the new parameters in eqn (3) and (4) we can obtain the soliton profiles for a DPPC membrane the in gel state, see Fig. 7. Both roots in eqn (4) are negatives, and

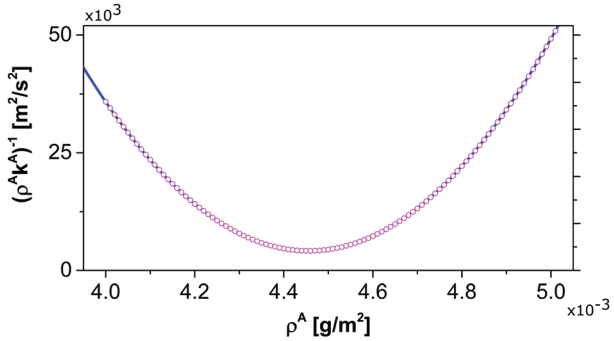

Fig. 6 Lateral sound velocity at low frequency as a function of the membrane area density. The blue line shows the data with ρ^A_{fluid} = 4.035 × 10^{-3} g m^{-2} at T = 45 °C.[12] Magenta circles display the data fitting with ρ^A_{gel} at $T < T_m$.

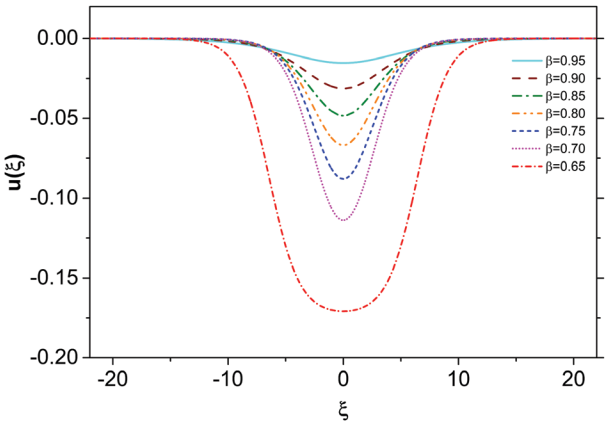

Fig. 7 Soliton profiles for DPPC at $T \approx$ 38 °C with different velocities, β.

the profiles are always negative because $\Delta\rho^A < 0$. The maximum lateral density change possible in the model is:

$$\Delta\rho^A_{max} = \frac{|p|}{q}. \quad (5)$$

Considering the membrane in the gel phase and according to the parameters (p and q) found by us, the maximum lateral density is 0.174 (17%). This change corresponds to ≈71% of the total area change in the transition of DPPC, which is ≈25%.[21] In this work, is not possible to calculate the lateral sound velocity as a function of membrane area density because the experimental data are insufficient. Although we have measured the heat capacity profile, we ignore the lateral density values for our lipid membranes.

4 Conclusion

As mentioned in the Introduction, the evidence of mechanical changes in the membrane linked to the action potential was shown by Iwasa and Tasaki.[2,3] The authors also discussed the relationship between the propagation of a nerve impulse and changes in the membrane temperature. The H–H model fails to explain these thermodynamic phenomena and therefore new points of view have emerged to explain the changes in the membrane during the action potential.[42,43]

In the lipids of artificial and biological membranes, the thermodynamic features are closely linked to volume and area changes.[11,21] The phase transition causes changes in the membrane thickness and lateral pressure, and the heat capacity and compressibility increase reaching a maximum at T_m. A soliton model proposes the propagation of an isentropic pulse near the phase transition[12] and its possible relation with mechanical dislocations along the membrane.

These are easily explored in lipid monolayers at the air–water interface and the existence of adiabatic sound waves has been studied by Griesbauer *et al.*[28,44] They reported a sound velocity of surface waves derived from k_s and ρ^A as well as the dependence of propagation of pulses on the state of the lipid monolayer.

This was also studied by Shrivastava *et al.*:[45] the fluorescence intensity of dye molecules embedded in a lipid interface is sensitive to phase transitions. The same group has recently shown two-dimensional solitary elastic pulses at an air–water interface.[30] In their experiments, they showed pulses propagating in the transition regime where the compressibility reaches a maximum. They varied the monolayer state by changing the surface density of lipid molecules, but it can also be modified by changing other physical features of the system.

Despite the facility of working with lipid monolayers, they do not represent a real biological system. A bilayer system is a more approximate model. Moreover, in lipid bilayers the surface density and lateral pressure are intrinsic to the final state. We found in this work that such a state can be locally modified by heat applied in a reduced zone of the bilayer. We suggest that as the lipids in this zone change from gel to fluid phase, a deformation is observed. This propagates along the membrane and eventually moves the laser target. How fast this perturbation travels is the next question we would like to answer in future work that is under progress, to hopefully confirm that it behaves as a soliton. For the time being, we have learnt here that a phase transition produced within a tiny region of a lipid membrane under water travels far away, suggesting that solitary waves may indeed propagate in nerves.

Conflicts of interest

There are no conflicts to declare.

Acknowledgements

This work has been supported by CONACYT, Mexico, under grants CB-220962 and FC-1132. M. I. P. C. acknowledges a scholarship from CONACYT. Fruitful discussions with Francisco Sierra, Victor Romero and Mauricio Castaño are acknowledged.

References

1 A. L. Hodgkin and A. F. Huxley, *J. Physiol.*, 1952, **117**, 500–544.
2 K. Iwasa and I. Tasaki, *Biochem. Biophys. Res. Commun.*, 1980, **95**, 1328–1331.
3 K. Iwasa, I. Tasaki and R. C. Gibbons, *Science*, 1980, **210**, 338–339.
4 G. H. Kim, P. Kosterin, A. L. Obaid and B. M. Salzberg, *Biophys. J.*, 2007, **92**, 3122–3129.
5 I. Tasaki, K. Kusano and P. M. Byrne, *Biophys. J.*, 1989, **55**, 1033–1040.
6 I. Tasaki, K. Kusano and P. M. Byrne, *Biochem. Biophys. Res. Commun.*, 1995, **215**, 654–658.
7 B. C. Abbott, A. V. Hill and J. V. Howarth, *Proc. Biol. Sci.*, 1958, **148**, 149–187.
8 J. V. Howarth, R. D. Keynes and J. M. Ritchie, *J. Physiol.*, 1968, **194**, 745–793.
9 K. Kaufmann, *On the role of the phospholipid membrane in free energy coupling*, Brasil, Caruaru, 1st edn, 1989.
10 K. Kaufmann, *Action potentials and electrochemical coupling in the macroscopic chiral phospholipid membrane*, Brasil, Caruaru, 1st edn, 1989.
11 H. Ebel, P. Grabitz and T. Heimburg, *J. Phys. Chem. B*, 2001, **105**, 7353–7360.
12 T. Heimburg and A. D. Jackson, *Proc. Natl. Acad. Sci. U. S. A.*, 2005, **102**, 9790–9795.
13 T. Heimburg, *Thermal Biophysics of membranes*, Wiley-VCH Verlag, Weinheim, Germany, 2007.
14 K. R. Srinivasan, R. L. Kay and J. F. Nagle, *Biochemistry*, 1974, **13**, 3494–3496.
15 N. I. Liu and R. L. Kay, *Biochemistry*, 1977, **16**, 3484–3486.
16 E. Evans and R. Kwok, *Biochemistry*, 1982, **21**, 4874–4879.
17 D. Needham and E. Evans, *Biochemistry*, 1988, **27**, 8261–8269.
18 P. L.-G. Chong, R. Ravindra, M. Khurana, V. English and R. Winter, *Biophys. J.*, 2005, **89**, 1841–1849.
19 J. Nagle and D. Wilkinson, *Biophys. J.*, 1978, **23**, 159–175.
20 J. F. Nagle, *Biophys. J.*, 1993, **64**, 1476–1481.
21 T. Heimburg, *Biochim. Biophys. Acta, Biomembr.*, 1998, **1415**, 147–162.
22 A. Blicher, K. Wodzinska, M. Fidorra, M. Winterhalter and T. Heimburg, *Biophys. J.*, 2009, **96**, 4581–4591.
23 S. Mitaku and T. Date, *Biochim. Biophys. Acta, Biomembr.*, 1982, **688**, 411–421.
24 C. S. Spyropoulos, *Am. J. Physiol.*, 1961, **200**, 203–208.
25 H. Tyäuble, M. Teubner, P. Woolley and H. Eibl, *Biophys. Chem.*, 1976, **4**, 319–342.
26 W. H. Moolenaar and I. Spector, *J. Physiol.*, 1979, **292**, 297–306.
27 Y. Kobatake, I. Tasaki and A. Watanabe, *Adv. Biophys.*, 1971, **2**, 1–31.
28 J. Griesbauer, S. Bössinger, A. Wixforth and M. F. Schneider, *Phys. Rev. Lett.*, 2012, **108**, 198103.
29 O. Albrecht, H. Gruler and E. Sackmann, *J. Phys.*, 1978, **39**, 301–313.
30 S. Shrivastava and M. F. Schneider, *J. R. Soc., Interface*, 2014, **11**, 20140098.
31 S. Shrivastava, K. H. Kang and M. F. Schneider, *Phys. Rev. E: Stat., Nonlinear, Soft Matter Phys.*, 2015, **91**, 012715.
32 M. Montal and P. Muller, *Proc. Natl. Acad. Sci. U. S. A.*, 1972, **69**, 3561–3566.
33 T. McIntosh, S. Simon and R. MacDonald, *Biochim. Biophys. Acta, Biomembr.*, 1980, **597**, 445–463.
34 J. Pope and D. Dubro, *Biochim. Biophys. Acta, Biomembr.*, 1986, **858**, 243–253.
35 K. Lohner, *Chem. Phys. Lipids*, 1991, **57**, 341–362.
36 M. Darvas, P. N. Hoang, S. Picaud, M. Sega and P. Jedlovszky, *Phys. Chem. Chem. Phys.*, 2012, **14**, 12956–12969.
37 B. Fabian, M. Darvas, S. Picaud, M. Sega and P. Jedlovszky, *Phys. Chem. Chem. Phys.*, 2015, **17**, 14750–14760.
38 T. Brumm, K. Jørgensen, O. Mouritsen and T. Bayerl, *Biophys. J.*, 1996, **70**, 1373–1379.
39 V. P. Ivanova and T. Heimburg, *Phys. Rev. E: Stat., Nonlinear, Soft Matter Phys.*, 2001, **63**, 041914.
40 L. S. J. M. Berg and J. L. Tymoczko, *Biochemistry*, W. H. Freeman, New York, 2002.

41 B. Lautrup, R. Appali, A. D. Jackson and T. Heimburg, *Eur. Phys. J. E: Soft Matter Biol. Phys.*, 2011, **34**, 1–9.
42 R. Appali, S. Petersen and U. van Rienen, *Adv. Radio Sci.*, 2010, **8**, 75–79.
43 R. Appali, U. van Rienen and T. Hemimburg, *A comparison of the Hodgkin-Huxley model and the soliton theroy for the action potential in nerves*, Academic Press, 2012, vol. 16, pp. 275–279.
44 J. Griesbauer, A. Wixforth and F. Schneider, *Biophys. J.*, 2009, **97**, 2710–2716.
45 S. Shrivastava and M. F. Schneider, *PLoS One*, 2013, **8**, e67524.